Hindawi
International Journal of Photoenergy
Volume 2019, Article ID 7492453, 7 pages
https://doi.org/10.1155/2019/7492453

*Research Article*

# The Synthesis of 2D $CH_3NH_3PbI_3$ Perovskite Films with Tunable Bandgaps by Solution Deposition Route

**Vorrada Loryuenyong**,[1,2] **Pajaree Thongpon**,[1] **Sasathorn Saudmalai**,[1] **and Achanai Buasri**[1,2]

[1]*Department of Materials Science and Engineering, Faculty of Engineering and Industrial Technology, Silpakorn University, Nakhon Pathom 73000, Thailand*
[2]*Center of Excellence on Petrochemical and Materials Technology, Chulalongkorn University, Bangkok 10330, Thailand*

Correspondence should be addressed to Vorrada Loryuenyong; vorrada@gmail.com

Received 11 September 2018; Accepted 4 December 2018; Published 7 February 2019

Guest Editor: Hui Wang



Nowadays, organo-lead halide is one of the most interesting materials for perovskite solar cells. This is because of its ease of fabrication, long absorption wavelength region, and long diffusion length. In this study, we investigated the bandgap tuning of hybrid mixed-halide perovskite films. The films were prepared by sequential two-step deposition technique, using 5-ammonium valeric acid iodide (5-AVAI), $PbI_2$, and a mixture of $CH_3NH_3I$ and $CH_3NH_3Br$ as precursor solutions. The results confirmed the formation of 2D perovskites in the presence of 5-AVAI. The obtained films had higher moisture resistance, better surface coverage, and smaller grain size, compared to the films without 5-AVAI. With the introduction of $Br^-$ ions, the change in the lattice parameter was observed. The bandgap was also found to increase with increasing $Br^-$ content.

## 1. Introduction

Perovskite solar cells have currently gained a prominent attention in the academic community and in the solar cell industry. It is the fastest advancing energy technology in the world, growing from an efficiency of just 3.8% in 2009 [1] to over 22% in 2017 [2]. The only major concern in the field of perovskite research is the stability of the devices and the use of lead in perovskite compounds. For the latter issue, lead alternatives have been proposed to be used in perovskite solar cells. However, the power conversion efficiency of such devices is still significantly behind lead-based devices.

A perovskite structure is anything that has the generic form $ABX_3$, where A is a large atomic or an organic cation (i.e., $CH_3NH_3^+$ and $CH(NH_2)_2^+$), B is a positively charged cation (i.e., $Pb^{2+}$ and $Sn^{2+}$), and X is a smaller atom which is negatively charge (anion) (i.e., $Cl^-$, $I^-$, and $Br^-$). In the case of perovskite solar cells, the most efficient devices so far have been produced with the 3-dimensional (3D) organic-inorganic halide perovskite, in which $CH_3NH_3^+$ as an organic cation, $Pb^{2+}$ as a big inorganic cation, and halide ions such as $Cl^-$ and $I^-$ as slightly small anions. Such perovskite materials can be made of cheap raw materials in a relatively simple manufacturing process. Additionally, they possess interesting optical and electronic properties including broad absorption spectrum, fast charge separation, long charge and exciton diffusion length, long carrier separation lifetime, and tunable bandgap.

The drawbacks of this material is that it is an ionic crystal and unstable against moisture. Previous researches have shown that there are several reaction pathways leading to degradation such as the reactions with water and oxygen and even the diffusion of electrode materials [3]. To improve the resistance to moisture, several approaches have been made in all areas of perovskite processing, including mixed-phase perovskites and two-dimensional (2D) perovskite structures [4, 5].

While the best perovskite structures with high and uniform qualities of the deposited films have been fabricated

with vacuum deposition methods, such processes are complicated. Low-temperature solution deposition routes, on the other hand, offer a much simpler process. Recent improvements to device solution-based processing have led to significant increases in the surface coverage while reducing the surface roughness [6, 7]. In this study, we investigated the possibility to tune the energy bandgap of mixed-cation perovskite in the presence of ammonium valeric acid iodide (5-AVAI). A combination of $Br^-$ halide ions was also incorporated into the perovskite structure, using precursor solutions of $CH_3NH_3I$ and $CH_3NH_3Br$ with various molar ratios.

## 2. Materials and Methods

*2.1. Materials.* Lead iodide ($PbI_2$) was purchased from Aldrich Chemistry. Methylammonium iodide ($CH_3NH_3I$ (MAI)), methylammonium bromide ($CH_3NH_3Br$ (MABr)), 5-ammonium valeric acid iodide ($C_5H_{12}INO_2$ (5-AVAI)), and fluorine-doped tin oxide (FTO) conductive glass substrates (TEC8, 8 Ω/square) were purchased from Dyesol. N,N-Dimethylformamide (DMF) and 2-propanol were purchased from Ajax Finechem Pty Ltd. All chemicals were commercially available and used without further purification.

*2.2. Precursor Preparation.* $MAI_xBr_y$ precursor (10 mg/ml) was prepared by mixing various molar ratios (100 : 0, 75 : 25, 50 : 50, 25 : 75, and 0 : 100) of MAI and MABr in 2-propanol. 0.95 ml 1 M $PbI_2$ and 0.05 ml 1 M 5-AVAI (5% 5-AVAI) in DMF were mixed together under stirring at 70°C.

*2.3. Film Preparation.* Fluorine-doped tin oxide (FTO) conductive glass substrates with dimensions of 2.5 cm × 2.5 cm were first cleaned with distilled water, ethanol, and acetone and then dried in an oven at 70°C. The perovskite films were then prepared by the sequential two-step deposition technique. 20 μl of mixed $PbI_2$+5-AVAI solution was first introduced onto the FTO substrates by spin-coating at 3000 rpm for 30 s under ambient condition. After annealing at 70°C for 10 min, a $MAI_xBr_y$ precursor solution (~200 μl) was subsequently spin-coated on top at 3000 rpm for 30 s. This step was repeated 5 times to ensure an excess supply of organic precursors for complete reactions of perovskite films. The films were finally annealed at 70°C for 20 min.

*2.4. Characterization.* XRD analyses of perovskite films were performed using a Shimadzu XRD-6100 diffractometer with Cu Kα radiation ($\lambda = 0.154056$ nm, 40 kV, and 30 mA). The optical properties were measured by ultraviolet-visible (UV-vis) absorption spectra (UV-1800, Shimadzu). The energy bandgap was calculated using the Tauc plots [8] of $(\alpha E) = A(E - E_g)^{1/2}$, where $\alpha$ is the absorption coefficient, $E$ is energy, $E_g$ is energy bandgap, and $A$ is a constant. Raman spectra were obtained using a Bruker Senterra Infinity 1 Raman microscope. Field-emission scanning electron microscopy (FE-SEM) (Mira3, Tescan) was employed to determine the surface morphologies of the perovskite films. All of the samples were gold coated to ensure good electrical conductivity. For the moisture stability test, all the perovskite films were put into a container, in which the air humidity was held

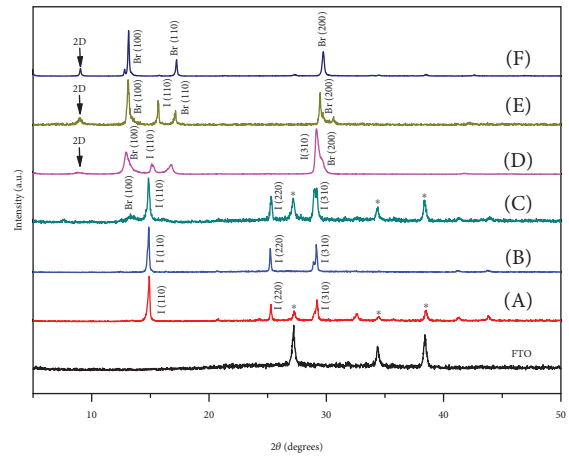


Figure 1: XRD patterns of $MAPb(I_{1-x}Br_x)_3$ prepared from MAI +MABr precursor solution at various molar ratios: (A) 100 : 0 w/o 5-AVAI; (B) 100 : 0; (C) 75 : 25; (D) 50 : 50; (E) 25 : 75; and (F) 0 : 100. (I = $MAPbI_3$, Br = $MAPbBr_3$, * = FTO).

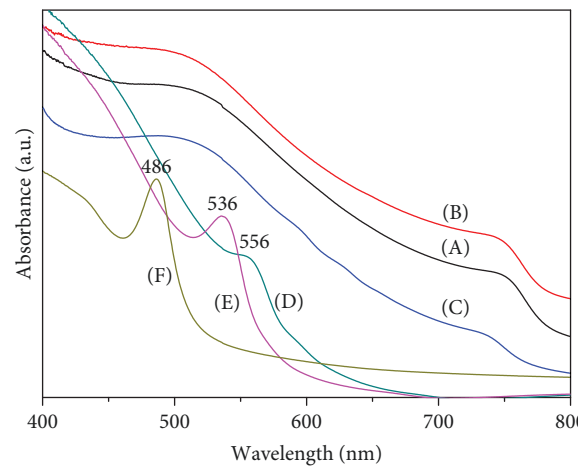


Figure 2: Absorption spectra of $MAPb(I_{1-x}Br_x)_3$ prepared from MAI +MABr precursor solution at various molar ratios: (A) 100 : 0 w/o 5-AVAI; (B) 100 : 0; (C) 75 : 25; (D) 50 : 50; (E) 25 : 75; and (F) 0 : 100.

constant by employing a beaker filled with saturated salt solutions. The salt, NaCl, was used for controlling the humidity level to 75% relative humidity (RH). All experiments were performed at room temperature.

## 3. Results and Discussion

In this research, 5% 5-AVAI was used for film preparation. Generally, the introduction of 2D perovskites into 3D counterparts has been shown to enhance the environmental stability to the 3D structure. This is because 2D perovskites are formed on the 3D perovskite grains to passivate interfacial defects and vacancies and enhance moisture resistance [9]. Previous researches have reported that the addition of a suitable amount of bulky organic cations, i.e., 5-AVA cations, between the anionic layers to induce the formation of 2D perovskites would result in smoother 2D perovskite layers with a better coverage, which is one of the possible reasons to improve the stability of perovskite films [5, 10]. Based on

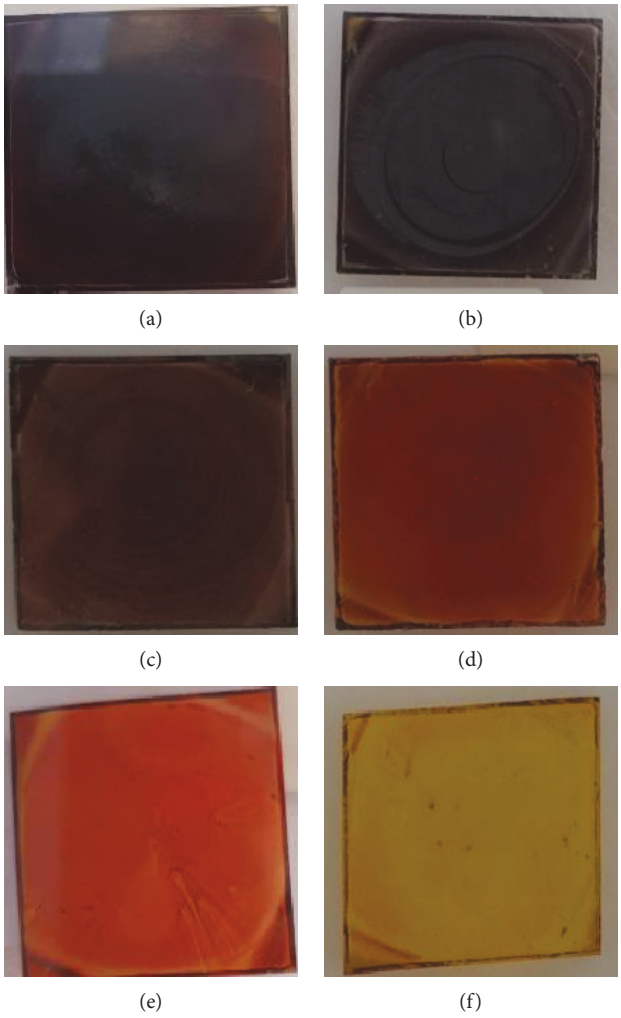


Figure 3: Photographs of $MAPb(I_{1-x}Br_x)_3$ prepared from MAI +MABr precursor solution at various molar ratios: (a) 100 : 0 w/o 5-AVAI; (b) 100 : 0; (c) 75 : 25; (d) 50 : 50; (e) 25 : 75; and (f) 0 : 100.

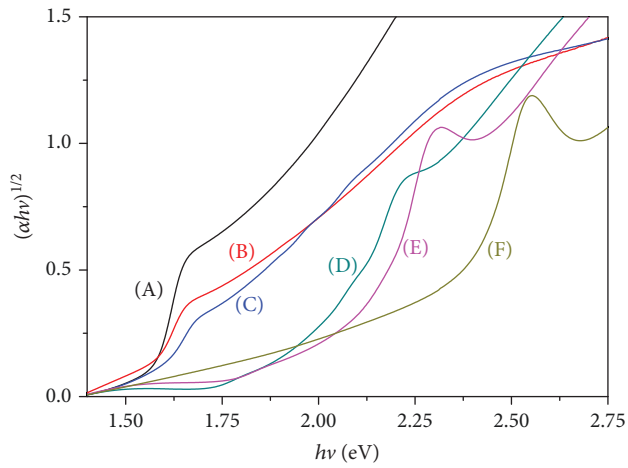


Figure 4: Tauc plots of $MAPb(I_{1-x}Br_x)_3$ prepared from MAI+MABr precursor solution at various molar ratios: (A) 100 : 0 w/o 5-AVAI, (B) 100 : 0, (C) 75 : 25, (D) 50 : 50, (E) 25 : 75, and (F) 0 : 100.

Table 1: Absorption edge and bandgap of $MAPb(I_{1-x}Br_x)_3$ prepared from MAI+MABr precursor solution at various molar ratios.

| MAI : MABr | Absorption edge (nm) | Bandgap (eV) |
|---|---|---|
| 100 : 0 (w/o 5-AVAI) | 793 | 1.56 |
| 100 : 0 | 793 | 1.56 |
| 75 : 25 | 780 | 1.59 |
| 50 : 50 | 601 | 2.06 |
| 25 : 75 | 574 | 2.17 |
| 0 : 100 | 510 | 2.43 |

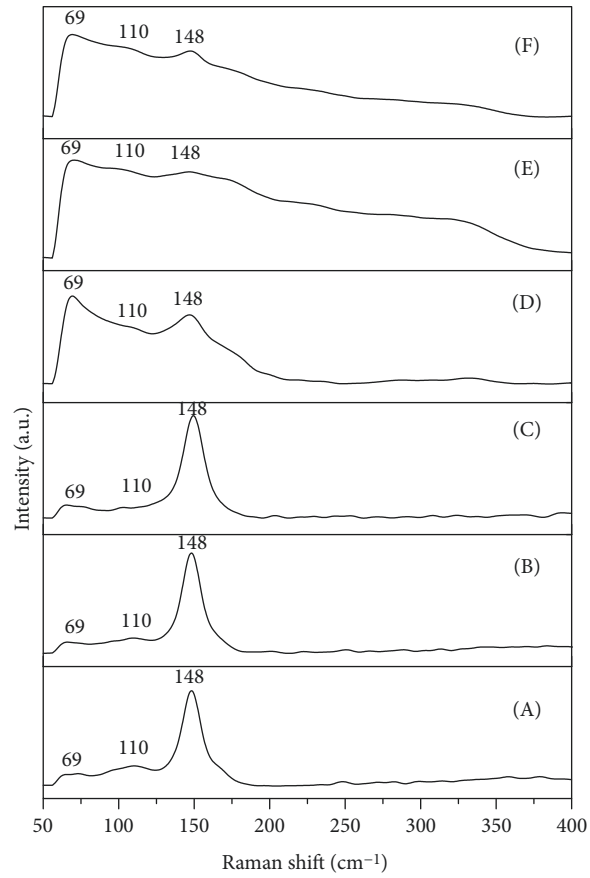


Figure 5: Raman spectra of $MAPb(I_{1-x}Br_x)_3$ prepared from MAI +MABr precursor solution at various molar ratios: (A) 100 : 0 w/o 5-AVAI, (B) 100 : 0, (C) 75 : 25, (D) 50 : 50, (E) 25 : 75, and (F) 0 : 100.

our previous work, it has been found that 5% 5-AVAI was likely to be the optimized content for the preparation of 2D perovskite in 3D $MAPbI_3$ due to its uniform and smooth surface with no pinhole and complete surface coverage. In addition, perovskite films with 5% 5-AVAI addition have the bandgap matching with that of 3D $MAPbI_3$. At other 5-AVAI contents, the bandgap tended to slightly decrease.

Figure 1 presented the XRD patterns of the perovskite films. The traditional $MAPbI_3$ film (Figure 1(a)) clearly showed the three main peaks at 14.83°, 25.21°, and 29.13°, which could be indexed to the (110), (220), and (310) planes of tetragonal perovskite structure, respectively [11]. Similar

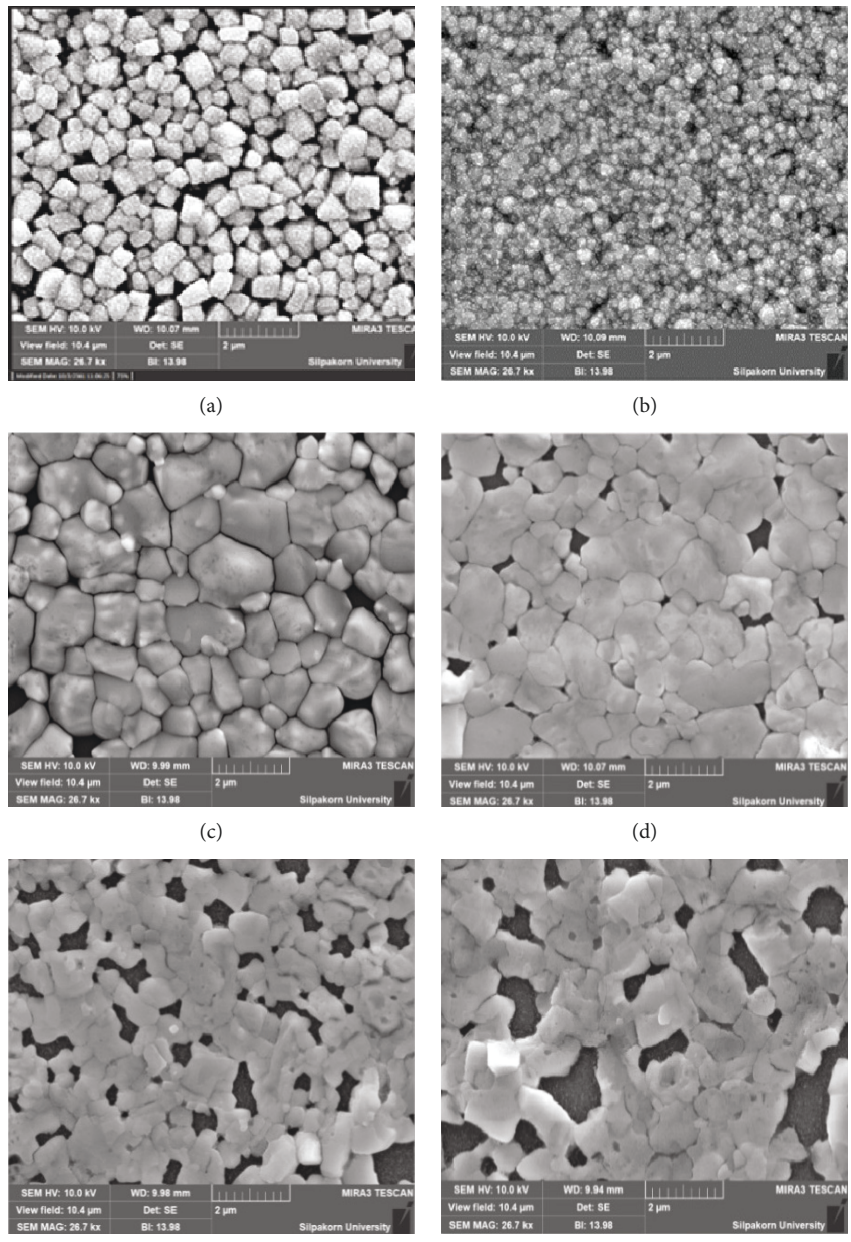


Figure 6: FE-SEM images of $MAPb(I_{1-x}Br_x)_3$ prepared from MAI+MABr precursor solution at various molar ratios: (a) 100 : 0 w/o 5-AVAI; (b) 100 : 0; (c) 75 : 25; (d) 50 : 50; (e) 25 : 75; and (f) 0 : 100.

XRD patterns were also observed for the 5-AVAI/MAI mixed perovskites (Figure 1(b)). With the addition of $Br^-$ ions in the precursor solution, the shift in XRD peaks to larger angles was observed, corresponding to a decrease in the lattice parameter. This could be due to the difference in the ionic radius of $Br^-$ and $I^-$ ions [12]. These films could, therefore, suffer from severe structural disorder and high density of traps. Nevertheless, no characteristic peak of $PbI_2$ was observed, illustrating that all $PbI_2$ was fully converted to perovskite crystals.

The XRD patterns of $MAPbBr_3$-rich perovskites (Figures 1(d)–1(f)) showed that it had a highly crystalline cubic phase. An additional diffraction peak at approximately 9.01° (marked with a black arrow), corresponding to the interlayer *d*-spacing of 9.7 Å, was also observed. This peak provided an evidence of the formation of a 2D perovskite layered structure [13]. This could be due to the relatively small ionic radius of $Br^-$ and the intercalation of the organic moiety from 5-AVAI, which allowed the formation of layered structure [5, 13]. In general, the perovskites made from mixed organic cations, especially with large 5-AVA cations, could produce a 2D layered structure [5]. Although no clear evidence of the peaks related to the 2D structure was observed for other films with 5-AVAI (Figures 1(b) and 1(c)), it might be because only a thin layer of 2D perovskite was formed, on top which a pure 3D perovskite was crystallized [5].

Figure 2 shows the absorption spectra of the films obtained by 5% 5-AVAI with various amount of $I^-$ : $Br^-$

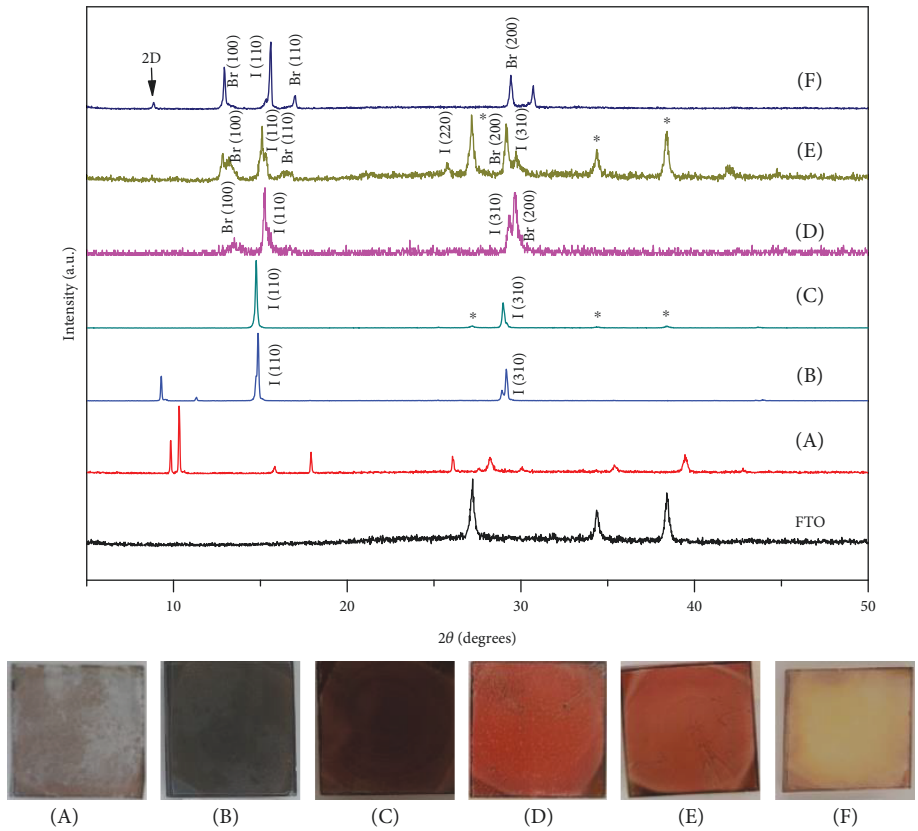


FIGURE 7: XRD patterns and photographs of degraded $MAPb(I_{1-x}Br_x)_3$ prepared from MAI+MABr precursor solution at various molar ratios: (A) 100 : 0 w/o 5-AVAI, (B) 100 : 0, (C) 75 : 25, (D) 50 : 50, (E) 25 : 75, and (F) 0 : 100. (I = $MAPbI_3$, Br = $MAPbBr_3$, * = FTO.)

ratios. For the $MAPbI_3$ perovskite with 5-AVAI addition (Figure 2(b)), the absorption band edge matched with that of 3D $MAPbI_3$ perovskite without 5-AVAI (Figure 2(a)). The absorption edges, however, were blue-shifted with increasing $Br^-$ content. For $MAPbBr_3$-rich perovskites (Figures 2(d)–2(f)), on the other hand, the prominent peaks at approximately 486-556 nm were observed. The peaks were also blue-shifted as the $Br^-$ content was increased. This was reported to be a result of exciton absorption attributed to the 2D quantum confinement [13]. Similar results were also observed for $PbI_2$ crystal intercalated with organic molecules [14]. Bandgap tunability of perovskite could be clearly seen from the photographs of deposited films (Figure 3). From the figure, the perovskite films turned from dark-red/black color to red color and finally to yellow color as the $Br^-$ content was increased.

In this study, it could be clearly observed that the bandgap of the perovskite could be tuned by varying the molar ratios of the mixed halide (MAI : MABr). The Tauc plots and calculated bandgap values were shown in Figure 4 and Table 1, respectively. A large bandgap variation from 1.56 to 2.43 eV was observed from 100 : 0 ($MAPbI_3$) to 0 : 100 ($MAPbBr_3$) molar ratios. The enlargement of bandgap with increasing $Br^-$ content could be due to a strong dependence of electronic energies on the effective exciton mass [15]. The above result was confirmed with a clear blue shift in the UV-vis absorption band edge in the absorption spectra as shown in Figure 2 and Table 1. The absorption onset of $MAPbI_3$ was located at 793 nm, while that of $MAPbBr_3$ thin film was blue-shifted to 510 nm.

Figure 5 compared the Raman spectra of the perovskite films obtained with laser excitation at 532 nm. For the films with low $Br^-$ content, the distinct peaks at 148 $cm^{-1}$ were observed, which could be assigned to the vibrational mode of the organic cation. The films also showed Raman peaks at 69 $cm^{-1}$ and 110 $cm^{-1}$, which were associated to the vibration modes of organic cations and $PbI_2$-layered crystal, respectively. For $MAPbBr_3$-rich perovskites (Figures 5(d)–5(f)), the films exhibited Raman broad bands at 50-200 $cm^{-1}$. These bands composed of a number of superimposed peaks, which were very similar to that of $PbI_2$ intercalated with organic molecules [15, 16], as discussed earlier. This result confirmed the presence of the 2D layered perovskite structure.

The effect of 5-AVAI and $Br^-$ ions on the morphology of the perovskite films was investigated by FE-SEM analysis. The surface FE-SEM images of all the perovskite films were shown in Figure 6. It could be seen that the tightly compact perovskite crystals with free pinhole and smaller grain size were obtained with the incorporation of 5-AVAI. This could be due to the promotion of perovskite nucleation by the bulky 5-AVA cations. No needle-like $PbI_2$ structures were observed in the films, confirming that $PbI_2$ was fully converted into perovskite, as discussed in XRD analysis. With

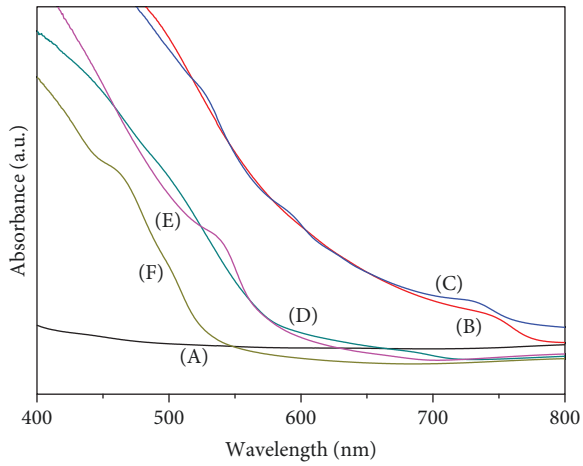


Figure 8: Absorption spectra of the degraded $MAPb(I_{1-x}Br_x)_3$ prepared from MAI+MABr precursor solution at various molar ratios: (A) 100 : 0 w/o 5-AVAI; (B) 100 : 0; (C) 75 : 25; (D) 50 : 50; (E) 25 : 75; and (F) 0 : 100.

increasing $Br^-$ content, larger grain size and pinholes were observed. Previous works [11, 17] has shown that methylammonium bromide (MABr) solution could induce Ostwald ripening process, converting the $MAPbI_3$ films into high-quality $MAPb(I_{1-x}Br_x)_3$ perovskite films with large grain size. Larger pinholes could be a result of distorted structure and the incomplete perovskite formation. It was found that both MAI and MABr could not dissolve together very well in DMF solvent. This would cause high reaction rate of the perovskite crystals, resulting in thin films with pinhole formation and incomplete surface coverage [18].

Figure 7 shows the XRD patterns and the film quality after exposure to air for 9 days at a controlled humid environment (75% RH). For the films with 5-AVAI (Figures 7(b)–7(f)), the crystalline nature was still confirmed. The films still remained intact, although the films experienced color fading. For films prepared without 5-AVAI, after a 9-day exposure in air, the color was changed from dark-red/black to slightly brown/colorless. This was different than what have been previously reported, in which the films turned to yellow color due to the film degradation to $PbI_2$ when reacting with moisture. In addition, the films showed remarkable change in the intensity of characteristic perovskite XRD peaks. Additional peaks at 8.83° and 9.33° were observed, which corresponded to the (001) and (100) planes of colorless monohydrate $CH_3NH_3PbI_3{\cdot}H_2O$, respectively. Such monohydrate phase is generally an intermediate product, which could be driven to form the dehydrate and finally the $PbI_2$ upon prolonged exposure to water vapor [19]. The presence of this phase could then confirm the moisture instability of the perovskite films without 5-AVAI addition. The stability of the films with 5-AVAI was additionally confirmed with light absorption behavior of the films, as shown in Figure 8. Without 5-AVAI addition, the absorbance of the film degraded completely, indicating the film degradation under relative humidity of 75% RH. The absorbance, however, still remained stable in the films with 5-AVAI, although a decrease in an intensity of excitonic peaks from 2D structure was observed.

## 4. Conclusions

In conclusion, we reported the formation of 2D mixed organic-halide perovskite with tunable bandgap and good moisture resistance. The bandgap of perovskite films could be tuned from 1.56 eV to 2.43 eV by replacing $I^-$ ions with smaller $Br^-$ ions. However, the film quality was degraded with the introduction of $Br^-$ ions. This could be due to incomplete dissolution of mixed MAI and MABr precursor solutions. The results, however, could be useful for the development of the graded structure of perovskite, allowing the possible development of hole conductor-free solar cells or efficient light absorbers for perovskite solar cells.

## Data Availability

The data used to support the findings of this study are available from the corresponding author upon request.

## Conflicts of Interest

The authors declare that there is no conflict of interest regarding the publication of this paper.

## Acknowledgments

The authors wish to thank the Department of Materials Science and Engineering, Faculty of Engineering and Industrial Technology, Silpakorn University, for supporting and encouraging this investigation.

## References

[1] A. Kojima, K. Teshima, Y. Shirai, and T. Miyasaka, "Organometal halide perovskites as visible-light sensitizers for photovoltaic cells," *Journal of the American Chemical Society*, vol. 131, no. 17, pp. 6050-6051, 2009.

[2] W. S. Yang, B.-W. Park, E. H. Jung et al., "Iodide management in formamidinium-lead-halide–based perovskite layers for efficient solar cells," *Science*, vol. 356, no. 6345, pp. 1376–1379, 2017.

[3] N. Rajamanickam, S. Kumari, V. K. Vendra et al., "Stable and durable $CH_3NH_3PbI_3$ perovskite solar cells at ambient conditions," *Nanotechnology*, vol. 27, no. 23, article 235404, 2016.

[4] D. Zhou, T. Zhou, Y. Tian, X. Zhu, and Y. Tu, "Perovskite--based solar cells: materials, methods, and future perspectives," *Journal of Nanomaterials*, vol. 2018, Article ID 8148072, 15 pages, 2018.

[5] G. Grancini, C. Roldán-Carmona, I. Zimmermann et al., "One-year stable perovskite solar cells by 2D/3D interface engineering," *Nature Communications*, vol. 8, article 15684, 2017.

[6] J. Burschka, N. Pellet, S.-J. Moon et al., "Sequential deposition as a route to high-performance perovskite-sensitized solar cells," *Nature*, vol. 499, no. 7458, pp. 316–319, 2013.

[7] M. Becker and M. Wark, "Recent progress in the solution-based sequential deposition of planar perovskite solar cells," *Crystal Growth & Design*, vol. 18, no. 8, pp. 4790–4806, 2018.

[8] M. A. Green, K. Emery, Y. Hishikawa, W. Warta, and E. D. Dunlop, "Solar cell efficiency tables (version 48)," *Progress in Photovoltaics*, vol. 24, no. 7, pp. 905–913, 2016.

[9] T. M. Koh, V. Shanmugam, X. Guo et al., "Enhancing moisture tolerance in efficient hybrid 3D/2D perovskite photovoltaics," *Journal of Materials Chemistry A*, vol. 6, no. 5, pp. 2122–2128, 2018.

[10] Z. Wang, Q. Lin, F. P. Chmiel, N. Sakai, L. M. Herz, and H. J. Snaith, "Efficient ambient-air-stable solar cells with 2D–3D heterostructured butylammonium-caesium-formamidinium lead halide perovskites," *Nature Energy*, vol. 2, no. 9, article 17135, 2017.

[11] M. Yang, T. Zhang, P. Schulz et al., "Facile fabrication of large-grain $CH_3NH_3PbI_{3-x}Br_x$ films for high-efficiency solar cells via $CH_3NH_3Br$-selective Ostwald ripening," *Nature Communications*, vol. 7, no. 1, article 12305, 2016.

[12] Y. Tu, J. Wu, Z. Lan et al., "Modulated $CH_3NH_3PbI_{3-x}Br_x$ film for efficient perovskite solar cells exceeding 18%," *Scientific reports*, vol. 7, no. 1, article 44603, 2017.

[13] R. Arai, M. Yoshizawa-Fujita, Y. Takeoka, and M. Rikukawa, "Orientation control of two-dimensional perovskites by incorporating carboxylic acid moieties," *ACS Omega*, vol. 2, no. 5, pp. 2333–2336, 2017.

[14] N. Preda, L. Mihut, M. Baibarac, M. Husanu, C. Bucur, and I. Baltog, "Raman and photoluminescence studies on intercalated lead iodide with pyridine and iodine," *Journal of Optoelectronics and Advanced Materials*, vol. 10, pp. 319–322, 2008.

[15] G. Bergamini and S. Silvi, Eds., *Applied Photochemistry: When Light Meets Molecules*, Springer, Cham, Switzerland, 2016.

[16] M. Ledinský, P. Löper, B. Niesen et al., "Raman spectroscopy of organic–inorganic halide perovskites," *Journal of Physical Chemistry Letters*, vol. 6, no. 3, pp. 401–406, 2015.

[17] V. Loryuenyong, N. Khiaokaeo, W. Koomsin, S. Thongchu, and A. Buasri, "Crystallisation of $CH_3NH_3PbX_3$ (X = I, Br, and Cl) trihalide perovskite using $PbI_2$ and $PbCl_2$ precursors," *Micro & Nano Letters*, vol. 13, pp. 486–489, 2018.

[18] J. Fan, B. Jia, and M. Gu, "Perovskite-based low-cost and high-efficiency hybrid halide solar cells," *Photonics Research*, vol. 2, no. 5, pp. 111–120, 2014.

[19] A. M. A. Leguy, Y. Hu, M. Campoy-Quiles et al., "Reversible hydration of $CH_3NH_3PbI_3$ in films, single crystals, and solar cells," *Chemistry of Materials*, vol. 27, no. 9, pp. 3397–3407, 2015.